

LV-2016-060



Landsvirkjun



Structural Drilling Targets from Platforms A, B, and F at Þeistareykir

Northern Rift Zone and Tjörnes Fracture Zone

LV-2016-060



Structural Drilling Targets from Platforms A, B, and F at Þeistareykir

Northern Rift Zone and Tjörnes Fracture Zone



ÍSOR-2016/030

Project no.: 16-0071

April 2016

Key Page**LV report no:** LV-2016-060 **Date:** April 2016**Number of pages:** 24 **Copies:** 10 **Distribution:** On www.lv.is
 Open
 Limited until**Title:** Structural Drilling Targets from Platforms A, B, and F at Þeistareykir. Northern Rift Zone and Tjörnes Fracture Zone**Authors/Company:** Maryam Khodayar, Sigurður Garðar Kristinsson and Ragna Karlsdóttir**Project manager:** Ásgrímur Guðmundsson (LV) Magnús Ólafsson (ÍSOR)**Prepared for:** Prepared by Iceland GeoSurvey (ÍSOR) for Landsvirkjun.**Co operators:**

Abstract: The purpose of this report is threefold. Firstly, we recall briefly the results of our three-year multidisciplinary structural analysis of Þeistareykir and surroundings for Landsvirkjun on which ground initial structural targets and areas were chosen for drilling. The base data include the extensive structural analysis of aerial images to shed light on the tectonic pattern, then the correlation with surface alteration and other results obtained by co-workers regarding the analysis of gases, resistivity, feeders in drilled wells, formation temperature, earthquakes 1993–2011, televiewer data, and to a lesser degree gravimetric and magnetic data. Secondly, we completed our investigations with an additional short analysis and correlation of the newest earthquakes from 2014–2015 recorded by the seismic network of ÍSOR-Landsvirkjun, as well as the latest mapped surface geothermal manifestations, and the production capacity. These correlations show the existence and the critical role of the Riedel shears of the transform zones, along with the rift, both in geological and geothermal processes. The role of the transform zone has not been demonstrated so strongly up to now. Finally, on the ground of these results, we suggest 2 drilling scenarios and several potential structural targets that include fault intersections and fault traces, to be drilled from platforms A, B, and F.

Keywords:

Northern Rift Zone; Tjörnes Fracture Zone; Structural drilling targets; Þeistareykir geothermal field; Tectonics.

ISBN no:**Approved by Landsvirkjun's
project manager**

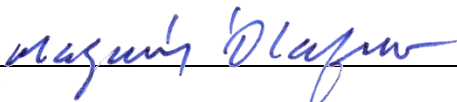
Project manager's signature 	Reviewed by SThor
--	----------------------

Table of contents

1	Introduction	7
2	The initial choice of structural targets	8
3	Revised structural targets for drilling	9
3.1	Brief correlation of new earthquakes and the fracture pattern	9
3.2	Production capacity and faults.....	10
3.3	Hot springs and surface geothermal manifestations	11
4	Structural targets to be drilled from platforms A, B & F	11
4.1	Scenario 1: Targets and wells from platforms A and B	12
4.2	Scenario 2: Targets and wells from platforms A, B, and F	12
5	References	15

List of figures

Figure 1.	<i>Recall of the results of the multidisciplinary structural analysis on which base the initial structural targets were chosen.</i>	17
Figure 2.	<i>Recall of basic parametres used for the structural analysis of fractures and feeders.</i> 18	
Figure 3.	<i>Recalling the fracture geometry. (a) Potential permeable fractures matching the feeders in each of the drilled wells. Example of possible fracture geometry and steep dips at depth, and relation to feeders: (b) Parallel segmented and non</i>	19
Figure 4.	<i>Recall of the initial suggested areas and structural targets for drilling</i>	20
Figure 5.	<i>Micro-earthquake activity of 2014–2015 recorded by ÍSOR-Landsvirkjun seismic network</i>	21
Figure 6.	<i>Production capacity, formation temperature and the distribution of the springs compared to the fracture pattern</i>	22
Figure 7.	<i>Scenario 1: Structural targets in area (a) to be drilled from platforms A, and B</i>	23
Figure 8.	<i>Scenario 2: Structural targets mostly in areas (a), (b) and (c) to be drilled from platforms A, B, and F</i>	24

1 Introduction

In 2012, ÍSOR suggested to Landsvirkjun a number of new wells at Þeistareykir based on geological, geophysical, and borehole data available at that time (Mortensen, 2012). Based on those results, wells were suggested from platforms A, B, C, and D.

From 2013 to 2015, ÍSOR undertook a thorough structural analysis of Þeistareykir geothermal field and its surroundings for Landsvirkjun (Khodayar and Björnsson, 2013; Khodayar, 2014; Khodayar et al., 2015a; 2015b). Þeistareykir geothermal field is at the junction of two types of plate boundaries (Fig. 1a), i.e., Northern Rift Zone (NRZ) and the Tjörnes Fracture Zone (TFZ), therefore, a highly fractured area. However, an up-to-date detailed tectonic pattern of both the rift and transform zones and their combined effects on geological and geothermal processes was not at hand. Additionally, newer data have been acquired since 2012. Therefore, our investigation used a multi-disciplinary approach to carry the structural analysis in which the following data were analysed and correlated together:

- Observations of aerial images (stereo pairs of aerial photographs, orthomaps and spot images) to identify the regional fracture patterns of both the rift and the transform zones.
- Tectonic control of surface alteration (Gíslason et al., 1984; Kristinsson et al., 2015), and own observations), as well as existing data on gases (Gíslason et al., 1984), resistivity (Karlsdóttir et al., 2012), magnetic and gravity data (Gíslason et al., 1984).
- Potential permeable fractures for feeders in boreholes (ÍSOR dataset).
- Brief correlation with stress field from Garcia et al. (2002) and Homberg et al. (2010).
- Addressing the shift of Þeistareykir fissure swarm.

Three of the main results of our investigation are: (a) Riedel shears of the transform zones were mapped in detail and they seem to be widespread at, and surrounding, Þeistareykir. (b) Although the fracture traces can in many cases be extremely subtle, their presence was also demonstrated by one or all of the other sets mentioned above. (c) The fractures belonging to the transform zone affect about any geological processes and the geothermal activity as much as the rift-parallel normal faults do, if not more in a few cases.

The ultimate goal of these investigations has been to use the new insights into the tectonics of this fractured reservoir in order to provide Landsvirkjun with some structural targets for drilling. In this respect, preliminary structural targets were provided along with the fracture geometry and assessment of stress conditions (Khodayar et al., 2015b). The purpose of this report is to provide a more considered choice of the structures and the approximate well paths from platforms A, B, and F reaching those structures.

In the following chapter, we first recall briefly the preliminary structural targets and the arguments for their identifications and choices. Then we present the chosen structures to be drilled from platforms A, B, and F as these are the immediate plans of

Landsvirkjun. The final choice of the structures take into account a few revisions, as well as the micro-earthquakes of 2014 and 2015 collected by the ÍSOR-Landsvirkjun seismic network (Ágústsson, 2016).

Finally, it is important to emphasize three points when using our suggestions for the structural drilling targets:

- Although many data are acquired, a conceptual model of the reservoir and its extent is not yet at hand to be used for well targeting.
- A part of the new results we obtained on the tectonics of Þeistareykir and surroundings is based on our direct observations and interpretations, but another part relies on measurements and results obtained in other studies up to the date of our analysis. If the base data regarding the formation temperature, borehole data, and gas measurements change, some of our structural interpretation should be revised along with the potential structural drilling targets.
- The initial ground for the renewed structural interpretation of Þeistareykir has been observations on aerial images, where major structures appear very clearly. But a portion of those observations concern young fractures and morpho-structural evidence, which are very subtle. That is the main reason why up to now many of those structures have been unnoticed. This is also why we undertook an additional and thorough multidisciplinary structural analysis to confirm the location and existence of the suggested fracture sets, a great part of which have subtle traces.

2 The initial choice of structural targets

The regional geology of Þeistareykir and results of our tectonic interpretations are thoroughly presented in our previous reports (e.g., Khodayar et al., 2015b). In this chapter, we recall briefly the data on which ground the initial structural targets were chosen:

- The analysis of formation temperature, feeders, surface alteration and distribution of gases above the reservoir, along with televiewer data from well ÞG-8 farther from the reservoir, revealed that these processes are controlled by the fracture sets belonging to both plate boundaries. The controlling fracture sets are dominantly the Riedel Shears of the transform zone (Fig. 1b), i.e., the ENE/NNE sinistral, as well as WNW and NW dextral oblique-slip faults, and to a lesser degree, the E-W although it is unknown if strike-slip motion is associated with the dip-slip of this set. Secondly, they are the northerly normal faults and open fractures of the rift. These initial structural targets consist of major structural boundaries and secondary parallel fractures. Among the major boundaries is a WNW segment to the north of Bæjarfjall (Fig. 1a). This segment is the splay of the WNW Stórhver-Bæjarfjall Fault on which the eruption of Stórhver has likely occurred. The Stórhver-Bæjarfjall Fault is also responsible for the shift of the Þeistareykir swarm in a dextral motion (Khodayar, 2014). Therefore, the

northerly structures to the north and south of this boundary are not likely to be same.

- Our structural interpretation of the resistivity data of Karlsdóttir et al. (2012) shows that the resistivity anomalies are controlled by the same tectonic structures and in the same locations as the structures suggested from aerial images and emerging from the above datasets (Fig. 1b). The tectonic structures controlling the resistivity anomalies present a rotation in the upper 8 km of the crust as presented in detail in our original report (Khodayar et al., 2015a). But in this study, figure 1c combines the tectonic structures controlling the resistivity anomalies of all depths in a single map along with other datasets as they reveal a good fit.
- From the above datasets we recall here the fractures that seem hosting the feeders in existing wells (Fig. 2), and recall also their segmented geometry and dips (Figs. 3a to 3k) as such fracture geometry and steep dips have implications for drilling.
- Finally, we proposed the initial targets both in terms of areas (Fig. 4a), and all of the potential tectonic fractures for drilling within them (Fig. 4b).

3 Revised structural targets for drilling

To suggest the present structural targets, we took into account few additional data in the final assessment of the structural targets. The additional data are:

- The micro-earthquakes of 2014 and 2015 from the ÍSOR-LV seismic network. A short correlation between the seismic lineaments and the structural pattern is also offered below.
- The active surface manifestations mapped by Kristinsson et al. (2015).
- Production capacities of wells, and potential permeable fractures in relation to the production capacities.

The revision also corrects one error regarding the labelling of the easternmost NS structure to the north of the main crater in Bæjarfjall. This short structure was labelled as “E” in our initial report (Khodayar et al., 2015b), meaning it was identified on the ground of gases. But the correct letter should have been “A”, indicating that this structure could be a possible boundary of Group 2 in formation temperature, although it is speculative as no well data is at hand yet in that location. The structure is now corrected on figures 1, 4, 7 and 8.

The present structural targets, after including the additional datasets, are presented in chapter 4 below.

3.1 Brief correlation of new earthquakes and the fracture pattern

The data recorded by the ÍSOR-Landsvirkjun seismic network indicate that 283 events occurred between January 2014 and December 2015, including 4 events between October and December 2013 (Fig. 5a). The focal mechanisms of these micro-earthquakes are not

at hand yet, but the seismic lineations have been shown in the report by Ágústsson (2016). On map, the majority of these earthquakes appear to be from north to the west of the main crater in Bæjarfjall. The depth of most of them is at 2 to 4 km in the crust, and their magnitude between 1 and 1.5 on Richter scale.

In our report of 2015 (Khodayar et al., 2015b) we pointed out that because the timing of these events coincided with the discharge of some of the wells at Þeistareykir, further investigation is needed to distinguish how many of these earthquakes result from natural release of stress in the crust, and how many are related to the discharge and testing of wells. As in both cases the underlying fractures are reactivated, and their strike and location are important for structural targets, we limit ourselves here to the interpretations of few seismic lineations and their correlation with the fracture pattern.

The majority of the seismic lineations in Bæjarfjall are to the south and west of well ÞG-4, and three fracture sets appear more obvious in the dataset (Fig. 5b). These are four parallel ENE, three other tightly parallel WNW, and one possible E-W seismic lineations. To recall, our structural analysis indicate that the ENE and WNW sets are respectively sinistral and dextral strike / oblique-slips, while the E-W set presents mostly dip-slip.

The interpreted seismic lineations and corresponding fractures are highlighted on figure 5b. These relocated earthquakes fit well with the suggested fracture traces, indicating that ruptures occurred on portions of these steeply dipping fracture segments.

3.2 Production capacity and faults

The production capacity estimated by Júlíusson (2015) is more thoroughly used here to gain additional insight into the Þeistareykir fractured reservoir in view of the final choice of the structural drilling targets. Figure 2 shows the production capacity of the 10 drilled wells along with the feeders and their potential permeable fractures in each well (Note that Fault 10, which is shown on figure 3a was missing from the original table presented on figure 2, but is now added to the table). Figure 3a summarises the identified fractures and the corresponding feeders on a map. However, some of these fractures were not included in our initial choice of structural targets (Fig. 4), because those targets were chosen as potential structural drilling targets that were not already crossed by previous wells.

Those fractures are included here on the map of the initial structural targets along with two additional information: (a) The production capacity is reported on the fault traces; (b) The formation temperature provinces (Khodayar et al., 2015b) are also used as a background.

The production capacity and formation temperature reveal interesting but unexpected correlation (Fig. 6a). The formation temperature of Group 2, representing the wells with boiling curve, is likely separated from Group 1 mostly by the ENE and the major WNW splay segment of the Stórhver-Bæjarfjall Fault that stretches from north of Tjarnarás to Bóndhóll. Although the extent of the formation temperature is unknown due to lack of wells away from the reservoir, a speculation was made that northerly fractures could also play a role in the compartmentalisation of formation temperature (Khodayar et al., 2015b). North of the WNW splay fault, the production capacity is 6.7 and southwest of

it between 7.3 and 10.2. Farthest south, the production capacity is the highest, or 20.9 (Fig. 6a). Both the highest and the lowest values fall within the area of Group 2 formation temperature (or boiling curve). This result is rather unexpected and may require additional investigation into formation temperature and or / production capacity.

3.3 Hot springs and surface geothermal manifestations

Finally, before suggesting structural targets from platforms A, B, and F, we reported the geothermal surface manifestations mapped by Kristinsson et al. (2015) on the fracture map (Fig. 6b). The high-temperature geothermal manifestations consist of springs, mud pots, solfataras, and fumaroles. They present a relatively good match with known fractures previously mapped around Tjarnarás, but also with our new structural interpretation where additional sets of fractures from the transform zone are identified.

In particular, the group of manifestations to the north of Bæjarfjall lines up on the trace of one of the ENE fracture segments we suggested. Other smaller groups of manifestations show an *en échelon* dextral arrangement exactly on the trace of the splay fault of the Stórhver-Bæjarfjall dextral fault. Some of the manifestations align on the NNE sinistral fault that we suggested down the west slope of Bæjarfjall, and others are on the trace of the northerly open fracture stretching from north of the main crater in Bæjarfjall to the northern slope of the mountain (Fig. 6b).

This correlation strengthens even more the previous results of our multidisciplinary structural analysis, which showed how the suggested rift and transform fracture sets control the geological and geothermal processes of Peistareykir and surroundings.

4 Structural targets to be drilled from platforms A, B & F

Several constraints played a role in the choice of the structural targets. Based on the results of our multidisciplinary structural analysis, area (a) is the most promising area for drilling, and some of the tectonic structures could act as boundaries between area (a) and the others. However, these boundaries are not proven yet. Therefore, the parts of areas (b), (c), (d), and (e) that are at the immediate border of area (a) also could be of interest for drilling.

As the focus is primarily on area (a), the main constraints for the choice of new structural targets there are that the area has a relatively small size (~ 4.5 km²) and hosts already the 10 drilled wells. Furthermore, as only half of platform A is available at the time of this study and the well head is already chosen, it dictate pretty much towards what direction the well path could go. This is also the case of platform (B) because the well site was already decided unrelated to the choice of structural targets. Finally, the selection of the targets is also influenced by the presence of existing well paths as they are to be avoided. Although these constraints are unrelated to the geological arguments for the selection of drilling targets, they dictate greatly our choices of the structural targets for further drilling.

Taking into account these constraints, we suggest two scenarios with a number of structural targets in each, which are primarily fracture intersections (Figs. 7 and 8). For

the wells, a maximum of 1 km length (view map) is considered. The choices of these targets are such that the wells: (1) Reach the highest expected fracture permeability where data also indicate potential heat and flow. (2) Interfere the least with the existing well paths. (3) Remain as much as possible in area (a) although some of these wells extend slightly into exploration areas (b) and (c) and additional information can be gathered about the reservoir for relatively low cost.

4.1 Scenario 1: Targets and wells from platforms A and B

In this scenario (Fig. 7), the structural targets are to be drilled only from platforms (A) and (B), as it is our understanding that Landsvirkjun wishes to start the drilling immediately from these two platforms. Two wells and five structures are suggested in scenario 1:

- **Well A1.** Only the northeastern part of the platform is built at the present. This dictate pretty much a well towards the east since wells PG-5 and PG-5b have already been drilled from that platform to the west and well PG-4 to the south (Fig. 7). The main target to the east is the intersection of the WNW fault (1) and the ENE fault (2). The WNW fault (1) is the splay fault of the Stórhver-Bæjarfjall main boundary (Khodayar and Björnsson, 2013; Khodayar et al., 2015a; 2015b), with a dextral oblique-slip motion, dipping to the southwest, likely steeply. The dip direction of fault (2) is unknown, but this ENE fault is parallel to sinistral Riedel shears that are widespread in all our analysed data. The advantage of well path A1 is that it remains in the hanging wall of fault (1) where deformation should be at a maximum and surface geothermal manifestations are concentrated.
- **Well B1.** The well path from platform (B) stretches southwards, crossing successively faults (1) and (2) while going through the favorable compartment between these two faults. The well path lies parallel to the northerly fault (3) and the ultimate target is the intersection of this fault with the ENE fault (5). The dip directions of faults (3) and (5) are unknown, but a few surface geothermal manifestations line on fault (5) and some on the trace of fault (3). On its path, the well also crosses the intersection of faults (3) and (4). Fault (4) is ENE and dips to the northwest and many surface manifestations seem aligned on the trace of this fault.

4.2 Scenario 2: Targets and wells from platforms A, B, and F

This scenario (Fig. 8) suggests a higher number of wells and well targets, some of which are options for a later stage. As before, the targets are mainly fracture intersections but fault traces outside of fault intersections are also considered.

The first immediate choices are:

- **Well A1.** The first well target is the intersection of the ENE fault (2) and the NS fault (4) to the east of platform (A). But on its way, the well goes also through the potentially good permeable compartment between the WNW splay fault (1) and the ENE fault 2 where the formation temperature follows the boiling curve

(Group 2) and surface geothermal manifestations are present. Up to this point, the well is about 500 m in length. Should Landsvirkjun wish to continue, a more southeasterly well path is suggested to cross successively portions of the ENE fault segments (5) and (6), the northerly fracture (7) and the EW fault (8). The structures (6), (7) and (8) are in area (b), which is an exploration area where resistivity anomalies indicate a possible upflow zone (Karlisdóttir et al., 2012). The dip directions of structures (6) and (7) are unknown, but the EW fault (8) dips northwards and is one of the two short segments with that strike in this locality.

- **Well B1.** The ultimate target of this well is the intersection of the WNW oblique-slip splay fault of Stórhver-Bæjarfjall (1) and the ENE fault (2). On its trace towards the ultimate target, the well crosses first the intersection of faults (1) and (3). Fault (3) dips to the northwest and has a normal-slip. As its NE strike is within the range of the sinistral Riedel shears of the transform zone, the fault could also have a strike-slip motion. It is assumed that the two motions of fault (3) provide the necessary permeability at the fault intersections with fault (1), where surface geothermal manifestations are also present on the hanging wall of the fault not so far from the intersection of faults (1) and (2).
- **Well F1.** A possible ENE short segment (fault 14) could act as the boundary between areas (a) and (c). Segment (14) is parallel to the ENE structures that were also seen on televiewer image logs below 1700 m in well PG-8. Well F1 stretches southwestwards parallel to segment (14), with the goal of reaching the intersection of the NW striking Tjarnarás fault system (faults 15) and the WNW splay fault (1). The two parallel NW segments dip to the southwest, have a normal-slip, and very likely a dextral strike-slip motion (Khodayar and Björnsson, 2013). Surface geothermal manifestations are between the two fault segments (15). Each of the NW faults (15), however, intersects fault (1) in a different place slightly apart. The first fault intersection is nearer to the trace of fault (14), but the ultimate target is slightly beyond the intersection of the westernmost NW fault (15) and fault (1) in a block that is the hanging wall of both the NW and WNW faults.

Additional choices for a later stage are:

- **Well B2** is a second choice from platform (B) and it targets the intersection of the WNW splay fault (1) with a possible fault segment striking ENE (13). Fault (13) dips to the southeast and surface geothermal manifestations are in the hanging wall of both of these faults. Well B2 crosses a part of the reservoir for which data is not at hand yet due to lack of drilling.
- **Well A2** is from the part of platform (A) that is not yet built. The suggested well path is towards the southeast, and the targets are the intersections of two northerly (11 and 12) and two ENE (9 and 10) faults, which have dip-slips. The strike of the northerly fractures is identical to the NNE sinistral Riedel shears of the transform zone, and the ENE faults are identified as having also a sinistral motion. Both of the northerly faults are eastward dipping, and both of the ENE faults southeastward dipping. Some seismic lineations seem to align on the ENE

faults (9) and (10) (Figure 5b). Due to the strike and dip-slip motions of the NNE and ENE faults, a good permeability is expected in the hanging walls of the two fault sets. Before reaching the targeted fault intersections, well A2 crosses a segment of fault (5), which dips northwestward and hosts surface geothermal manifestations. This interaction could also prove to be an interesting target.

Finally, we emphasize that the geometry and dip values of some of the suggested structural targets are unknown. But if they are similar to the faults that emerged from the structural analysis of the feeders, they are likely segmented at depth and have steep dips.

Acknowledgment. Our special thanks go to Ásgrímur Guðmundsson and Egill Júlíusson at Landsvirkjun for their support and project management. At ÍSOR, we thank Magnús Ólafsson for his excellent project management, and Sigvaldi Thordarson for a constructive review. We benefited greatly from discussions with Sveinbjörn Björnsson.

5 References

- Ágústsson, K. (2016). *Jarðskjálftavirkni á Þeistareykjum 2014 og 2015*. Iceland GeoSurvey, short report, ÍSOR-16005, 11 p.
- Garcia, S., Angelier, J., Bergerat, F., and Homberg, C. (2002). Tectonic analysis of an oceanic transform fault zone based on fault-slip data and earthquake focal mechanisms: the Húsavík-Flatey Fault zone, Iceland. *Tectonophysics*, 344, 157–174.
- Gíslason, G., Johnsen, G. V., Ármannsson, H., Torfason, H., and Árnason, K. (1984). *Þeistareykir: Yfirborðsrannsóknir á háhitasvæðinu*. National Energy Authority, report, OS-84089/JHD-16, 134 p., and 3 maps.
- Homberg, C., Bergerat, F., Angelier, J., and Garcia, S. (2010). Fault interaction and stresses along broad oceanic transform zone: Tjörnes Fracture Zone, North Iceland. *TECTONICS*, VOL. 29, TC1002, doi:10.1029/2008TC002415, 12 p.
- Júlíusson, E. (2015). *Álagsprófun á Þeistareykjum 2014–2015*. Landsvirkjun, short report 2014-403/08.02.04, 5 p.
- Karlsdóttir, R., Vilhjálmsson, A. M., Árnason, K., and Teklesenbet Beyene, A. (2012). *Þeistareykir Geothermal Area, Northern Iceland: 3D Inversion of MT and TEM Data*. Iceland GeoSurvey, report, ÍSOR-2012/046, 173 p. + CD.
- Khodayar, M. (2014). *Shift of Þeistareykir fissure swarm in Tjörnes Fracture Zone: Case of pull-apart on strike-slip?* Iceland GeoSurvey, report ÍSOR-2014/074, LV-2014-144, 21 p.
- Khodayar, M., and Björnsson, S. (2013). *Preliminary Fracture Analysis of Þeistareykir geothermal field and surroundings, Northern Rift Zone and Tjörnes Fracture Zone*. Iceland GeoSurvey, ÍSOR-2013/029. 57 p., 2 maps.
- Khodayar, M., Björnsson, S., Karlsdóttir, R., Ágústsson, K., and Ólafsson, M. (2015a). *Tectonic Control of Alteration, Gases, Resistivity, Magnetics and Gravity in Þeistareykir Area. Implications for Northern Rift Zone and Tjörnes Fracture Zone*. Iceland GeoSurvey, report ÍSOR-2015/002, LV-2015-039, 59 p., 2 maps.
- Khodayar, M., Björnsson, S., Kristinsson, S. G., Karlsdóttir, R., and Ólafsson, M. (2015b). *Multidisciplinary structural analysis and drilling targets at Þeistareykir, Northern Rift Zone and Tjörnes Fracture Zone*. Iceland GeoSurvey, report ÍSOR-2015/0043, LV-2015-0135, 49 p., 1 map.
- Kristinsson, S. G., Óskarsson, F., Ólafsson, M. and Óladóttir, A. A. (2015). *Háhitasvæðin á Þeistareykjum, Kröflu og Námafjalli. Vöktun á yfirborðsvirkni og grunnvatni árið 2015*. Iceland GeoSurvey, ÍSOR-2015/059, LV-2015-125, 175 p.
- Mortensen, A. K. (2012). *Þeistareykir: Tillögur um staðsetningu horholna í jarðhitakerfinu á Þeistareykjum 2012*. Iceland GeoSurvey, report ÍSOR-2012/043, 36 p.

Figures

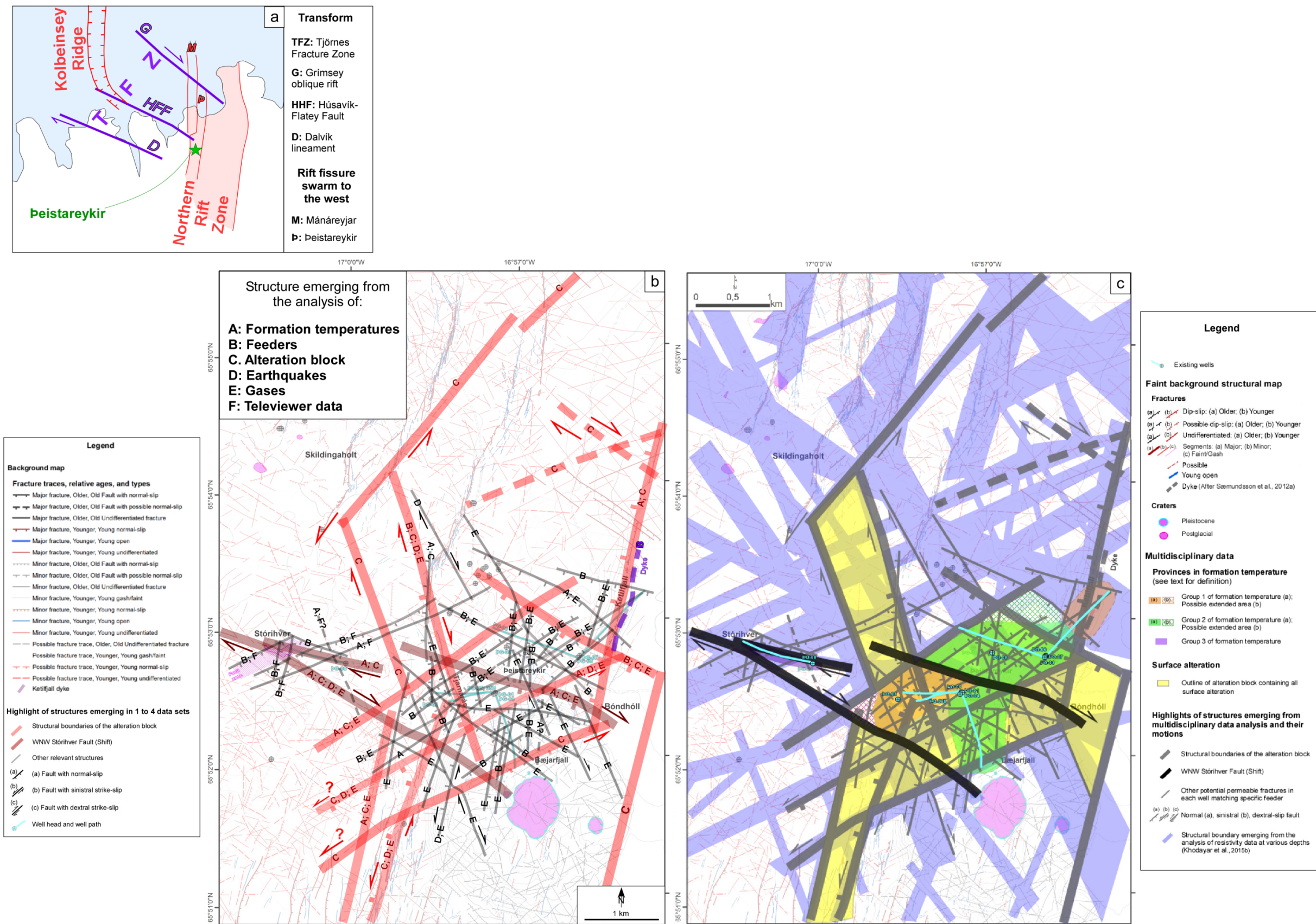


Figure 1. Recall of the results of the multidisciplinary structural analysis on which base the initial structural targets were chosen. (a) Simplified map showing the location of Peistareykir at the junction of rift and transform zone in North Iceland. (b) Highlight of critical structures playing a role in the geothermal processes as seen in six data sets. (c) Additional highlights of critical structures as seen in resistivity (modified from Khodayar et al., 2015b).

Well	Well type	Depth of the wells (TVD above sea level or from boreplatform)	Intersected fractures as suggested from this study (Figures 7 and 8)			Summary of intersected permeable fractures and feeders from this study	Depth of feeders (m) MD	Depth of feeders (m) TVD	Feeders in wells projected at the surface in terms of horizontal distance from well head	Mwe (Production capacity of the well)
			Horizontal distance of fractures to the feeder, projected on well path and presented as distance from well head	Strike of fractures	Dip of fractures	Fault numbers				
pG-01	V	1953 m (MD & TVD)	~ 110 m from feeder	N 67° E	If fault dips 80-85° SE (same fault as in pG-05?)	F 13	1620 m to 1640 m	1620 m to 1640 m	0 m	7.3
pG-05	I	1910 m (MD) 1627 m (TVD)	~ 210 m	N 67° E	If fault dips ~ 80-85° SE (same fault as pG-01?)	F 13	890 m	840 m	170	No Data
			~ 350 m	N 49° E	If fault dips 86° NW	F 10	1380 m to 1400 m	1275 m to 1295 m	440 to 460m	
pG-05B	I	2499 m (MD) 2369 (TVD)	~ 230 m	N 67° E	If fault dips 80°-85° SE (same fault as in pG-01; pG-05)	F 13	863 m	831	149 m	10.2
			~ 200 m	N165°E	If fault dips ~ 80-83° SW	F 12	1535 m	1445 m	365 m	
			~ 440 m	N158°E (Tjamarás Fault)	Fault dips 85°-87° WSW	F 11	2270 m	2165 m	~ 520m	
			~ 510 m	N 49° E	If fault dips 86° NW	F 10	2270 m	2165 m	~ 520m	
pG-02	V	1723 m (MD & TVD)	~ 30 m	N 156° E	If fault dips 85° WSW	F 9	657 m, 960 m, 1062 m	657 m, 960 m, 1062 m	0 m	No Data
			~ 50 m	N 55° E	If fault dips ~ 85° NW	and / or F7	657 m, 960 m, 1062 m	657 m, 960 m, 1062 m	0 m	
			~ 80 m	N 53° E	If fault dips ~ 85° SE	and / or F6	960 m, 1062 m	960 m, 1062 m		
			~ 15 m	N 00° E	If fault dips ~ 85° W	and / or F8	657 m, 960 m, 1062 m	657 m, 960 m, 1062 m		
pG-04	I	2240 m (MD) 1870 m (TVD)	~ 420 m	N 08° E	If fault dips ~ 80° E	F 14	1600	1390 m	600	20.9
			~ 680 m	N 54° E	If fault dips 85° SE	F 15	1840	1603 m	770 m	
			~ 680 m	N 132° E	If fault dips 85° SW	and / or F16	1840	1603 m	770 m	
pG-07	I	2509 m (MD) 2069 m (TVD)	Sub-parallel to pG-07 at the surface; ~ 70 m of feeder	N 50° E	If fault dips ~ 85° NW	F 25	750 m	721 m	135 m	4.1
			~ 290 m	N116° E	If fault dips ~ 85° SW	and / or F26	750 m	721 m	135 m	
			~ 890 m	Dyke of Ketilfjall: N 15°-20° E	If dyke dips ~ 82° E	DYKE 29	2325 m to 2345 m	1955 m to 1970 m	1105 to 1115m	
			~ 1190 m	N101° E	If fault segments dip ~ 85° SW and NE	and / or F28	2325 m to 2345 m	1955 m to 1970 m	1105 to 1115m	
pG-03	V	2659 m (MD & TVD)	~ 50 m	N 20° E	If fault dips 85°- 87° W	F 27	1610 m to 1680 m, 1880 m	1610 m to 1680 m, 1880 m	0 m	6.7
			~ 50 m	N 50° E	If fault dips 85°-87° NW (same as in pG-07?)	and / or F25	1610 m to 1680 m, 1880 m	1610 m to 1680 m, 1880 m		
pG-06	I	2799 m (MD) 2456 m (TVD)	~ 220 m	N 54° E	If fault dips 85° SE	F 23	846 m	811 m	165 m	6.7
			~ 420 m	N 40° E	If fault dips 85° SE	F 22	1145 m	1098 m	315 m	
			~ 580 m	N 57° E	If fault dips 85° NW	F 21a	1720 m to 1740 m	1578 m to 1595 m	605 to 615m	
			~ 720 m	N 04° E	If fault dips 85° E	and / or F19	1720 m to 1740 m	1578 m to 1595 m	605 to 615m	
			~ 930 m	N 06° E	If fault dips 85° W	F 18	2674 m	2380 m	1150m	
pG-09	V	2194 m (MD & TVD)	~ 80 m	N 02° E	If fault dips 85° W and is segmented at depth	F 20	860 m, 1460 m, 2100 m	860 m, 1460 m, 2100 m	0 m	3.5
			~ 90 m	N57° E	If fault segment dips 80°-85° SE (same fault as in pG-06)	and / or F21b	1460 m, 2100 m	860 m, 1460 m, 2100 m		
			~ 70 m	N117° E	If fault dips 80°-85° SW	and / or F24	860 m, 1460 m, 2100 m	860 m, 1460 m, 2100 m		
pG-08	I	2430 m (MD) 2220 m (TVD)	~ 550 - 850 m fault zone	N 69° E (in the fault zone)	Fault zone dipping 80°-83° SE	F 1	1680 m, 1748 m, 1773 m	1520 m, 1590 m, 1610 m	603, 640, 655m	No Data
			~ 750 m	N 06° E to N 20° E	If fault dips 80°-83° E	and / or F3	1680 m, 1748 m, 1773 m	1520 m, 1590 m, 1610 m		
			~ 550 - 850 m fault zone	N 67° E (in the fault zone)	Fault zone dipping 80°-83° SE	F 2a; 2b	1680 m, 1748 m, 1773 m; 2260 m	1520 m, 1590 m, 1610 m, 2040 m	870m	
			~ 900 m	N 11° E	If fault dips 80°-83° E	and / or F4	2260 m	2040 m		
			~ 150 m of feeders	N111° E (Stórhver dextral-oblique fault parallel to pG-08)	If fault dips 85° SW	and / or F5	1680 m, 1748 m, 1773 m; 2260 m	1520 m, 1590 m, 1610 m, 2040 m	603, 640, 655m & 870 m	

Figure 2. Recall of basic parameters used for the structural analysis of fractures and feeders. Well data and depths of the feeders are from the borehole reports (ÍSOR database), and the production capacity (MWe) is from Júlíusson (2015).

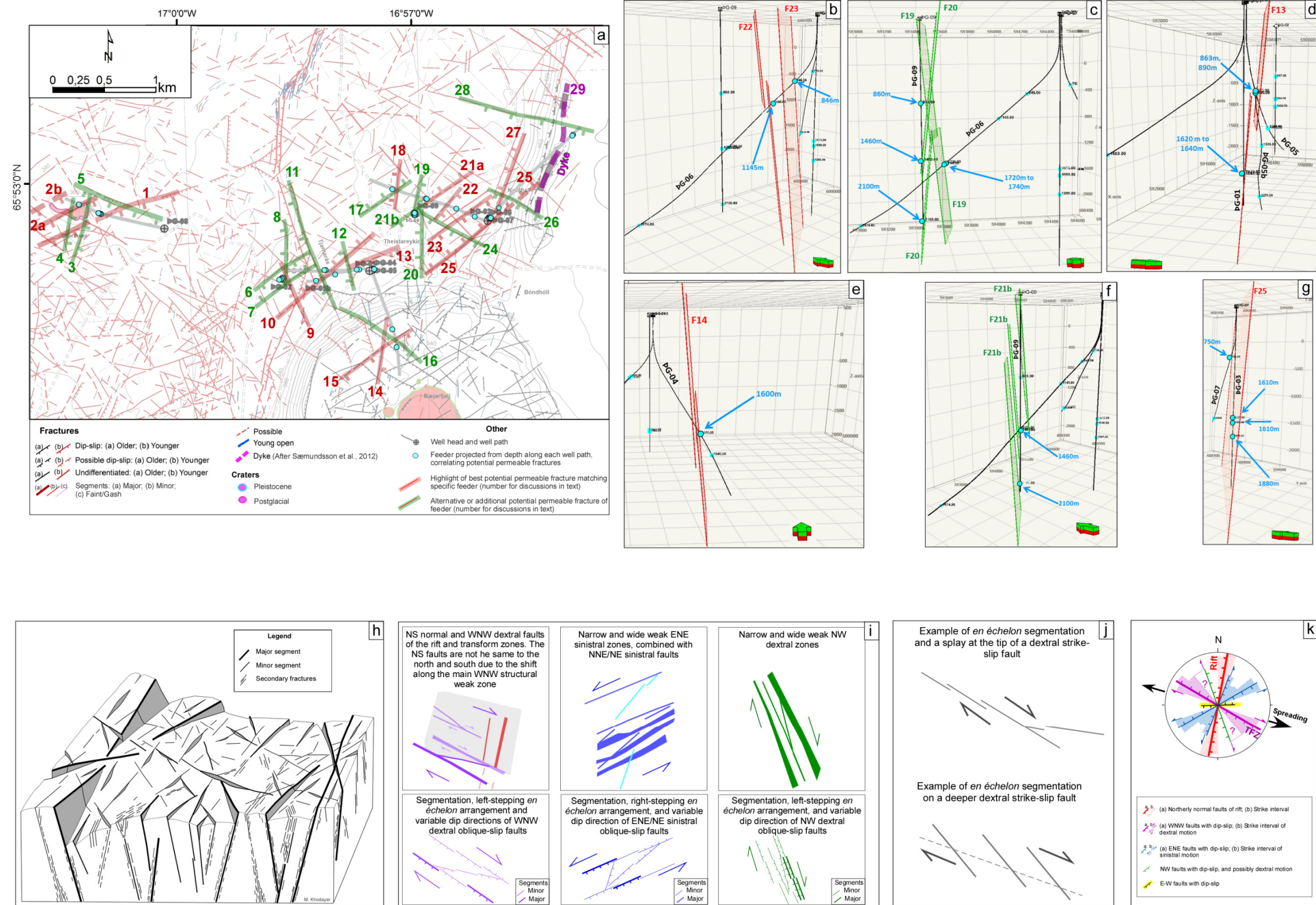


Figure 3. Recalling the fracture geometry. (a) Potential permeable fractures matching the feeders in each of the drilled wells. Example of possible fracture geometry and steep dips at depth, and relation to feeders: (b) Parallel segmented and non-segmented fractures. (c) Cross-cutting of segmented fractures. (d) Single segmented fractures. (e) Tightly parallel segments (f) Wider parallel segments. (g) Single steeply dipping fracture. (h) Block diagram of major and minor fractures in horizontal and vertical section. (i) View map of segmented and *en échelon* strike and oblique-slip fractures. (j) Further examples of *en échelon* arrangements and splay geometry on deeper fault. (k) Strike and motions of the fracture patterns of rift and transform zones compatible with the same direction of spreading direction (modified from Khodayar et al., 2015b).

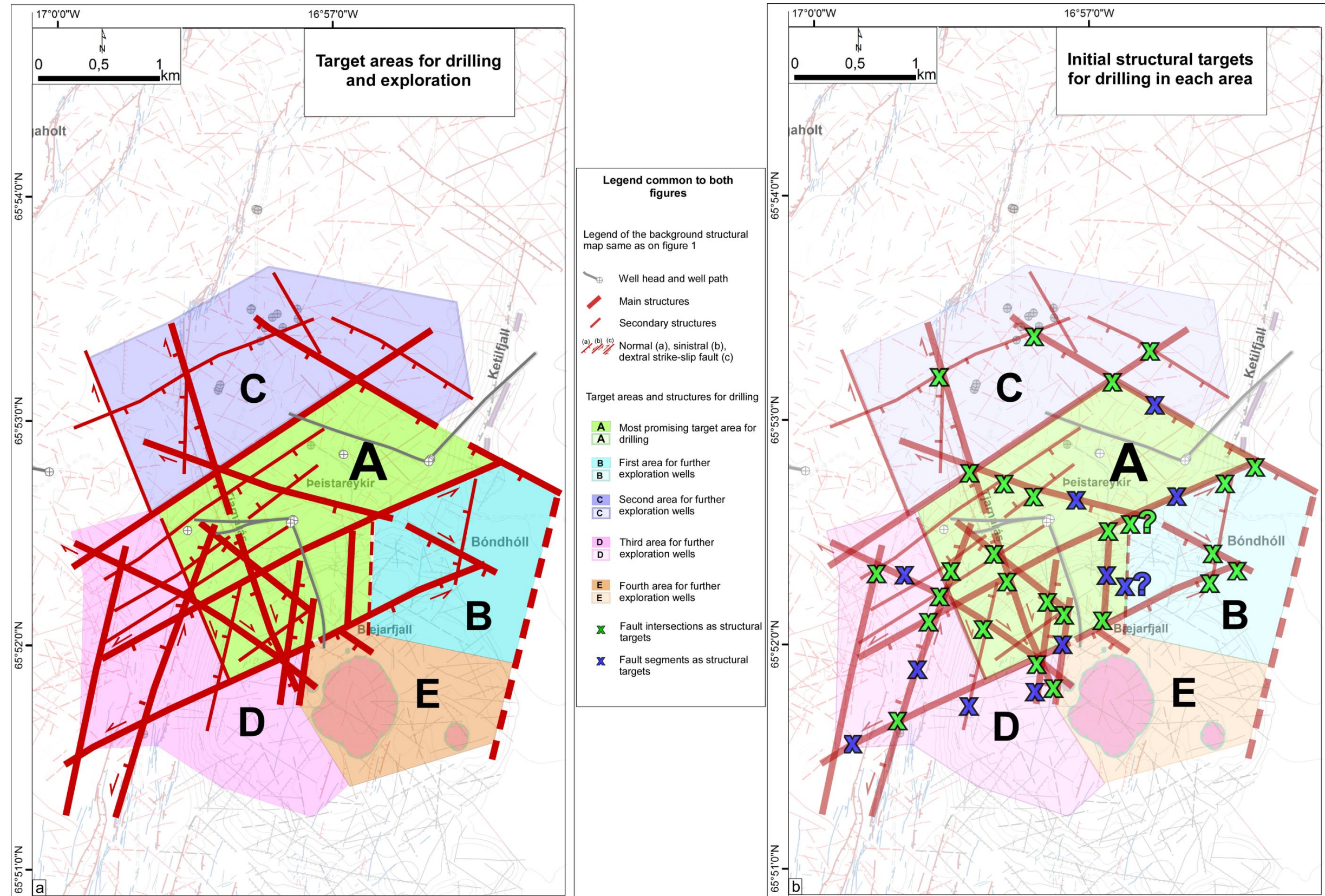


Figure 4. Recall of the initial suggested areas and structural targets for drilling. (a) The five suggested areas for drilling, where area (A) should provide Landsvirkjun with enough energy sought for the first stage of the power plant. Areas (B) to (D) are for further drilling exploration to provide additional information such as the size of the reservoir, the up-flow zone, and permeability at depth. (b) Structural targets belonging to rift and transform plate boundaries. The targets are mostly fracture intersections but also a few fracture traces, identified based on the multidisciplinary structural analysis (Khodayar et al., 2015a; 2015b).

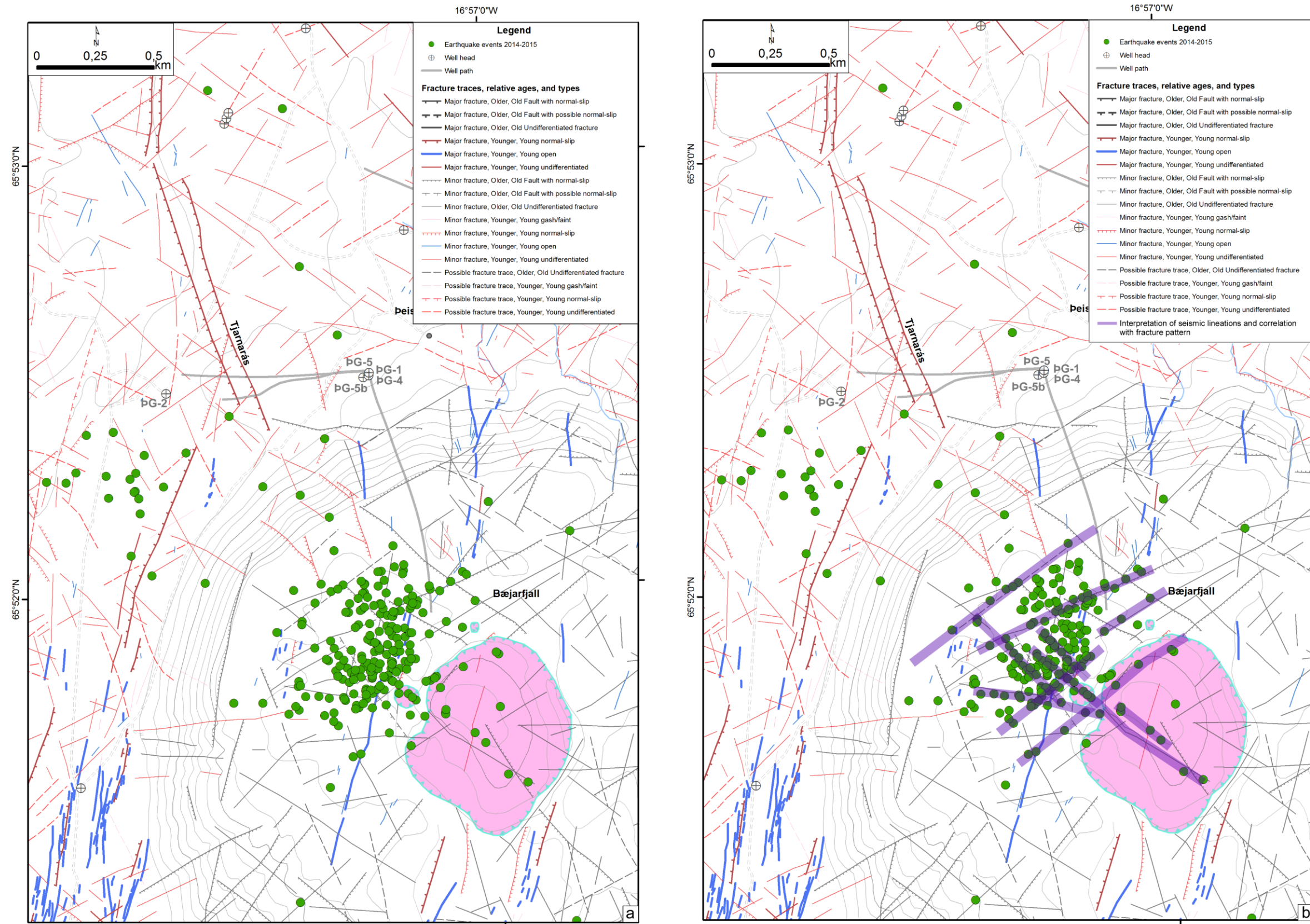


Figure 5. Micro-earthquake activity of 2014–2015 recorded by ÍSOR-Landsvirkjun seismic network. (a) Raw data reported on our structural map. (b) Interpretation of the most obvious seismic lineation shows a good fit with the suggested fractures.

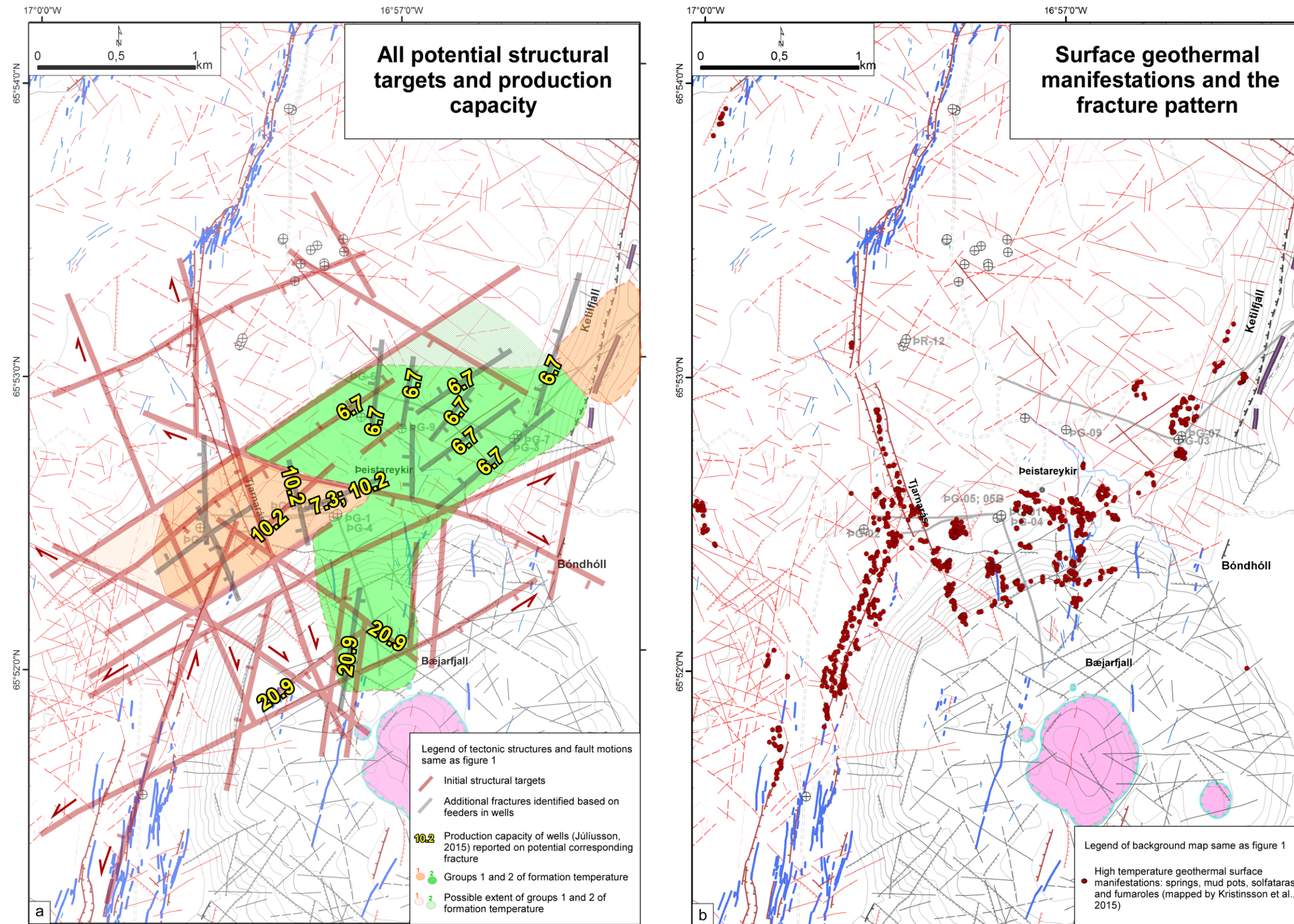


Figure 6. Production capacity, formation temperature and the distribution of the springs compared to the fracture pattern. (a) The initial structural targets are combined with the fractures identified through the structural analysis of feeders in the well. The known production capacity (Júliússon, 2015) are reported on the fractures and correlated with formation temperature (see text for explanation). (b) The surface geothermal manifestations (hot springs, solfataras, fumaroles) mapped in a separate investigation by Kristinsson et al. (2015) are superimposed on the fracture map of Khodayar and Björnsson (2013), showing a good match.

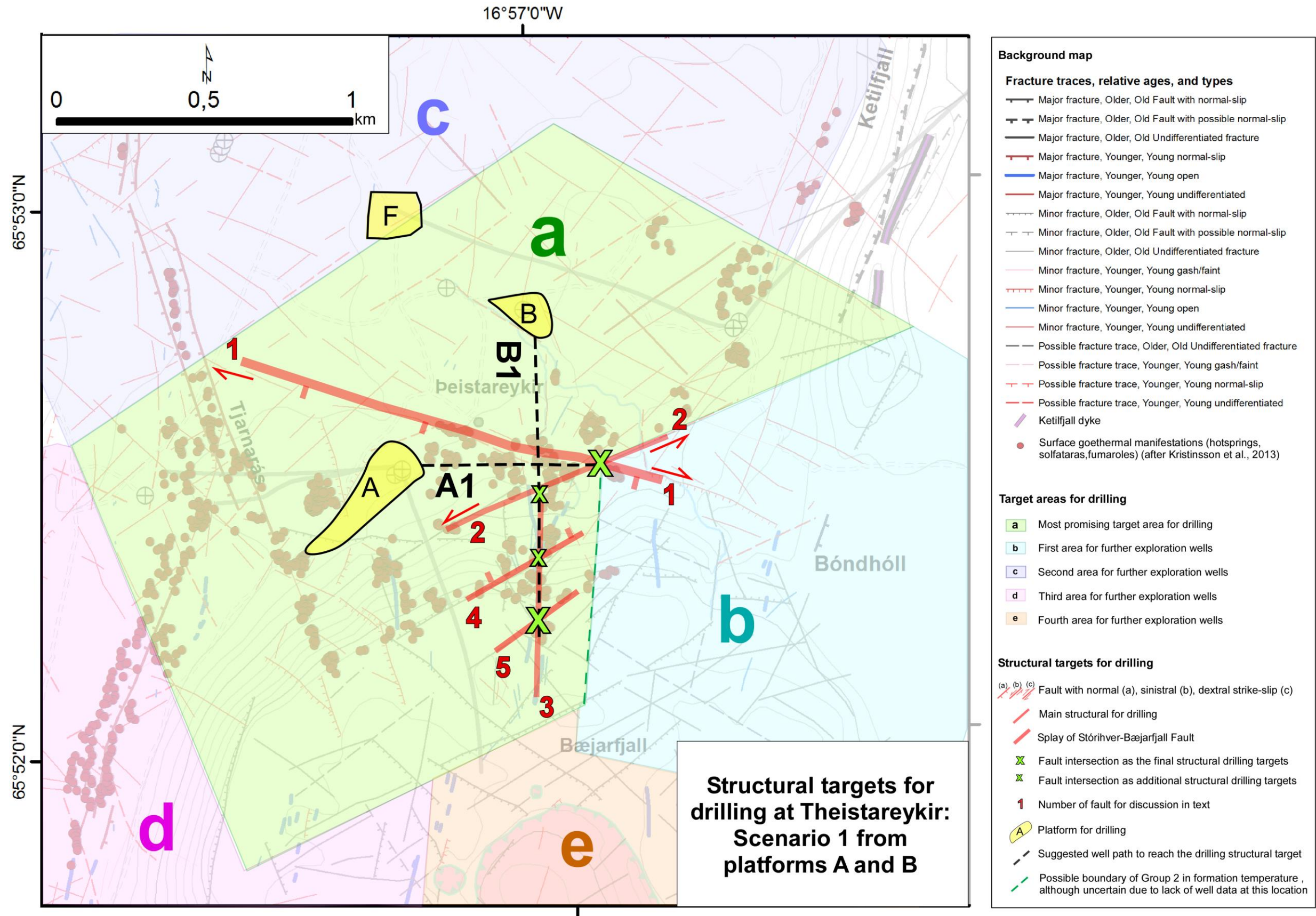


Figure 7. Scenario 1: Structural targets in area (a) to be drilled from platforms A, and B. See text for explanation.

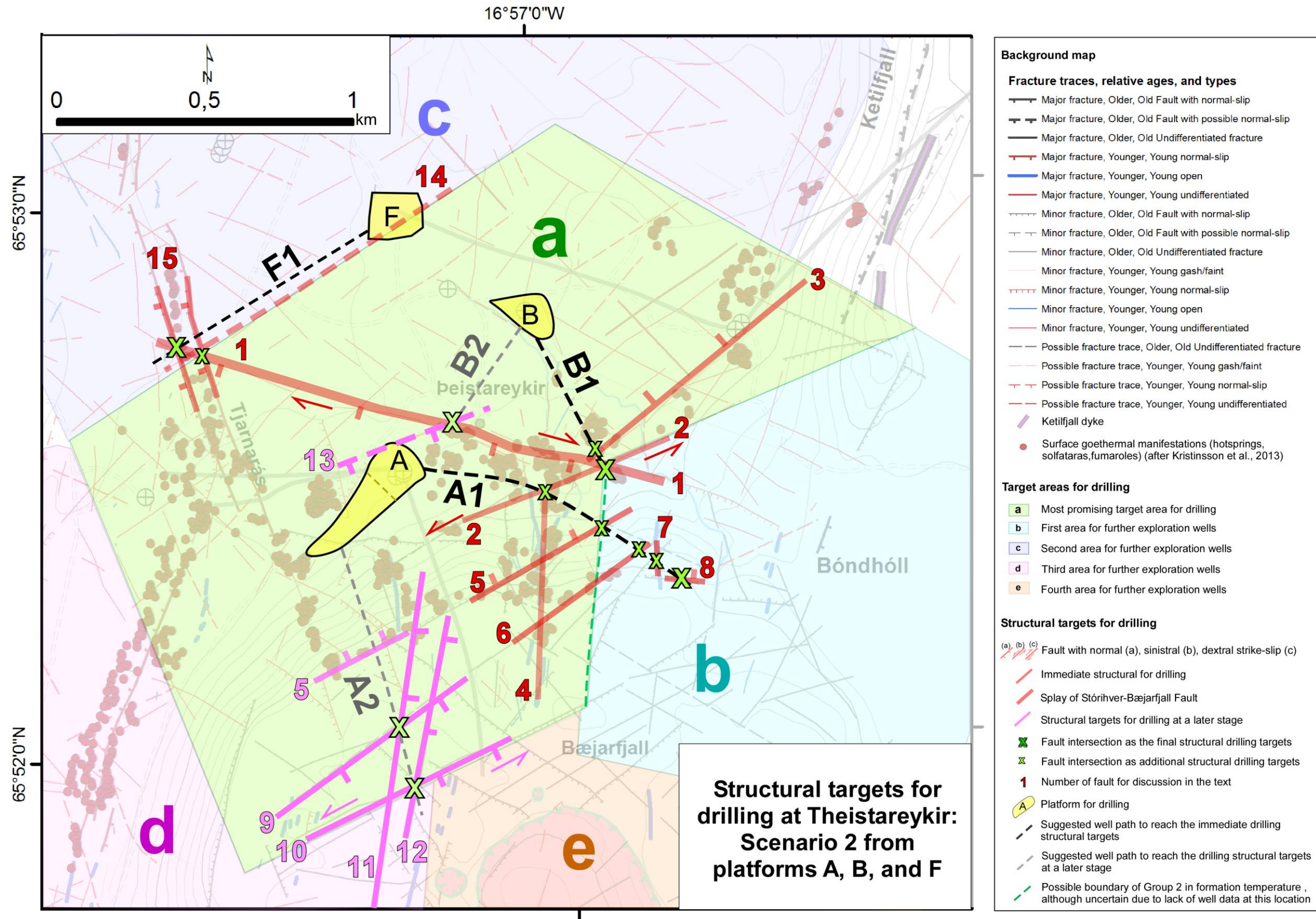


Figure 8. Scenario 2: Structural targets mostly in areas (a), (b) and (c) to be drilled from platforms A, B, and F. See text for explanation.